Inorganic Chemistry

Article

pubs.acs.org/IC

Three Isostructural One-Dimensional Ln^{III} Chains with Distorted Cubane Motifs Showing Dual Fluorescence and Slow Magnetic Relaxation/Magnetocaloric Effect

Yan Li,[†] Jia-Wen Yu,[‡] Zhong-Yi Liu,[‡] En-Cui Yang,*[,‡] and Xiao-Jun Zhao*[,†,‡]

[†]Department of Chemistry, Collaborative Innovation Center of Chemical Science and Engineering (Tianjin), Nankai University, Tianjin 300071, People's Republic of China

[‡]College of Chemistry, Key Laboratory of Inorganic−Organic Hybrid Functional Material Chemistry, Ministry of Education, Tianjin Key Laboratory of Structure and Performance for Functional Molecules, Tianjin Normal University, Tianjin 300387, People's Republic of China

Supporting Information

ABSTRACT: Three new homometallic lanthanide complexes with mixed carboxylate-modified rigid ligands, $[Ln(\mu_3\text{-OH})(na)(pyzc)]_n$ (na^- = 1-naphtholate, $pyzc^-$ = 2-pyrazinecarboxylate, Ln = Dy (**1**), Yb (**2**), and Gd (**3**)), were solvothermally synthesized, and their structures and magnetic as well as photophysical properties were completely investigated. Complexes **1**−**3** are crystallographically isostructural, exhibiting linear chains with four bidentate bridging μ-COO^- moieties encapsulated cubic $\{Ln_4(\mu_3\text{-OH})_4\}^{8+}$ clusters repeatedly extended by 4-fold chelating-bridging-$pyzc^-$ connectors. Magnetically, the former two complexes with highly anisotropic Dy^{III} and weak anisotropic Yb^{III} ions in the distorted NO_7 triangular dodecahedron coordination environment display field-induced slow relaxation of magnetization. Fitting the dynamic magnetic data to the Arrhenius law gives energy barrier $\Delta E/k_B$ = 39.6 K and pre-exponential factor $\tau_o = 1.52 \times 10^{-8}$ s for **1** and $\Delta E/k_B$ = 14.1 K and $\tau_o = 2.13 \times 10^{-7}$ s for **2**. By contrast, complex **3** with isotropic Gd^{III} ion and weak intracluster antiferromagnetic coupling shows a significant cryogenic magnetocaloric effect, with a maximum $-\Delta S_m$ value of 30.0 J kg^{-1} K^{-1} at 2.5 K and 70 kOe. Additionally, the chromophoric na^- and $pyzc^-$ ligands can serve as antenna groups, selectively sensitizing the Dy^{III}- and Yb^{III}-based luminescence of **1** and **2** in the UV−visible region by an intramolecular energy transfer process. Thus, complexes **1**−**3**, incorporating field-induced slow magnetic magnetization and interesting luminescence together, can be used as composite magneto-optical materials. More importantly, these interesting results further demonstrate that the mixed-ligand system with rigid carboxylate-functionalized chromophores can be excellent candidates for the preparations of new bifunctional magneto-optical materials.

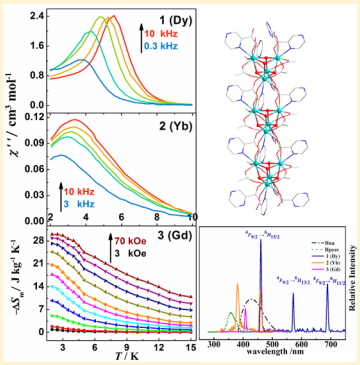

INTRODUCTION

The combination of various functions from different materials into a single compound has recently become a great interest for a broad range of applications as compared with those applicable materials with single performance.[1] Behaving as one of dual magneto-optical materials with both magnetic and luminescent properties, lanthanide coordination complexes with tailorable structures have drawn intense focuses due to their fascinating structures and potential applications in cryogenic magnetic refrigeration, high-density information storage, quantum computations,[1−3] MRI imaging, as well as cell labeling.[4] On one hand, resulting from the different local magnetic anisotropy and the large-spin multiplicity of the spin ground-state,[5,6] lanthanide complexes can act either as single-molecule magnets (SMMs),[7,8] especially for highly anisotropic Dy^{III}-based samples, or as low-temperature molecular magnetic coolers (MMCs) for isotropic Gd^{III}-containing entities.[9−11] Although opposite requirement for the single-ion anisotropy, both properties significantly depend on the interplay of the single-ion electron density and the crystal-field environment around the spin carrier.[12] Thus, for a given heavy lanthanide cation, synthetic chemists can design and create targeted magnetic materials through fine-tuning interactions between the spin carrier and crystal lattice generated by the functional coordination groups.

On the other hand, lanthanide complexes can also display well-separated, intense, narrow-line, and long-lived emissions in UV−visible and near-infrared (NIR) regions due to the presence of the luminescent lanthanide cations. However, the parity forbidden of the f → f transition makes the absorption coefficient much weaker. Fortunately, organic ligands with strongly absorbing chromospheres capable of transmitting the energy to the metal center can successfully resolve the obstacles,[13] which requires that the excited state of the ligand is higher in energy than that of the lowest excited state of the lanthanide cation.[5] Thus, it is of vital importance and a big challenge to construct dual magneto-optical materials to

Received: August 11, 2014
Published: December 18, 2014

   dx.doi.org/10.1021/ic501952b | Inorg. Chem. 2015, 54, 153−160

Table 1. Crystal and Structure Refinement Data for 1−3[a]

	1	2	3
empirical formula	$C_{16}H_{11}DyN_2O_5$	$C_{16}H_{11}N_2O_5Yb$	$C_{16}H_{11}GdN_2O_5$
F_w	473.77	484.31	468.52
cryst size [mm]	0.18 × 0.17 × 0.15	0.18 × 0.17 × 0.15	0.18 × 0.17 × 0.16
cryst syst	tetragonal	tetragonal	tetragonal
space group	$I\bar{4}$	$I\bar{4}$	$I\bar{4}$
a [Å]	18.9363(12)	18.885(7)	19.0364(14)
b [Å]	18.9363(12)	18.885(7)	19.0364(14)
c [Å]	8.2997(10)	8.222(3)	8.3437(12)
V [Å^3]	2976.1(4)	2932.3(19)	3023.6(5)
Z, D_c [g cm^{-3}]	8, 2.115	8, 2.194	8, 2.058
$h/k/l$	−22, 16/−22, 20/− 9, 9	−22, 16/−21, 22/− 9, 9	−22, 22/−22, 22/− 6, 9
$F(000)$	1816	1848	1800
μ [mm^{-1}]	5.052	6.409	4.417
reflections collected/unique	8693/2634	7742/2594	7792/2667
R_{int}	0.0435	0.0763	0.0168
data/restraints/params	2634/0/217	2594/127/217	2667/1/217
R_1[a], wR_2[b] [$I > 2\sigma(I)$]	0.0235, 0.0440	0.0357, 0.0897	0.0126, 0.0274
R_1, wR_2 [all data]	0.0246, 0.0445	0.0363, 0.0903	0.0132, 0.0276
max. and min transmission	0.7226 and 0.6608	0.4465 and 0.3917	0.5384 and 0.5036
GOF on F^2	1.050	1.082	1.029
$\Delta\rho_{max}$, $\Delta\rho_{min}$ [e·Å^{-3}]	0.557, − 0.515	1.937, − 2.714	0.293, − 0.290

[a] $R_1 = \Sigma(||F_0| - |F_c||)/\Sigma|F_0|$; [b] $wR_2 = [\Sigma w(|F_0|^2 - |F_c|^2)^2/\Sigma w(F_0^2)^2]^{1/2}$.

judiciously choose the functional organic connectors to effectively incorporate with the lanthanide cations. To date, lots of discrete oligomers with various metal coordination geometries (flat trigonal pyramid, trigonal bipyramidal,[14] distorted square-antiprismatic,[15] triangular dodecahedron, trigonal bipyramididal,[16] and so on), varying nuclearities (Dy_n (n = 3, 4, 5, 6, 26, 30) and Er_{26}), as well as polymeric multiple-dimensional frameworks with interesting core-topology (linear, planar triangles, seesaw, rhomb, zigzag) have been generated as applicable dual functional materials.[17−20] Surprisingly, the anisotropy barrier and the hysteresis temperature of these samples were greatly increased nearly 1200 and 370% as compared to the first SMM discovered in 1993.[12] Additionally, the enhanced NIR emissions and the prolonged lifetime of these lanthanide complexes modified by the bulky conjugate ligands have advanced the biological applications in bioimaging and cell labeling.[21]

Herein, to continue the structural-property investigations along the bifunctional materials, commercially available 1-naphthoic acid (Hna) and 2-pyrazinecarboxylic acid (Hpyzc) were selected as functional ligands to react solvothermally with different lanthanide cations. Generally, the carboxylate group-functionalized mixed ligands with chromophoric cores can serve as antenna groups and crystal-field adjustors to influence the luminescence and anisotropy of the lanthanide cations. As a result, three cubic tetranuclear cluster-based Ln^{III} complexes, $[Ln(\mu_3\text{-OH})(na)(pyzc)]_n$ (Ln = Dy (**1**), Yb (**2**), and Gd (**3**)) were successfully fabricated with satisfactory yields, and their structures, magnetic, and photophysical properties were investigated. Structurally, all the three examples exhibit slightly distorted cubane-shaped $\{Ln_4(\mu_3\text{-OH})_4\}^{8+}$ clusters with four bidentate bridging μ-COO^- encapsulations, which are extended into one-dimensional (1D) chains by 4-fold chelating-bridging $pyzc^-$ connectors. Magnetically, complexes **1** and **2** with highly anisotropic Dy^{III} and weak anisotropic Yb^{III} ions in the distorted NO_7 triangular dodecahedron coordination environment display field-induced slow magnetization relaxation to some different extent, in which $[Yb_4]$ cluster-based complex is scarcely observed to show such magnetic behavior. By contrast, complex **3** with isotropic Gd^{III} ion and weak antiferromagnetic coupling (J = −0.09 cm^{-1}) exhibits an obvious magnetocaloric effect (MCE) with a maximum value of $-\Delta S_m$ = 30.0 J kg^{-1} K^{-1} at 2.5 K and 70 kOe. Photoluminescence spectra of **1**−**3** suggest that the mixed carboxylate-functionalized rigid ligands can act as excellent antenna groups for effectively sensitizing the emissions of the lanthanide cations.

EXPERIMENTAL SECTION

All raw materials were commercially purchased from either Acros or Tianjin Chemical Reagent Factory and used as received without further purification. Doubly deionized water was used during the conventional synthesis. The instruments for typically physical measurements, the measurement procedures and conditions, and the X-ray crystallography[22−24] were described in the Supporting Information.

Synthesis of $[Dy(\mu_3\text{-OH})(na)(pyzc)]_n$ (1). $Dy(NO_3)_3{\cdot}6H_2O$ (45.7 mg, 0.1 mmol), Hna (34.4 mg, 0.2 mmol), Hpyzc (24.8 mg, 0.2 mmol), doubly deionized water (6.0 mL), and methanol (4.0 mL) were sealed in a Teflon-lined stainless steel vessel (23.0 mL), and the pH value of the mixture was adjusted to 5 by triethylamine with constant stirring. The resulting mixture was kept at 170 °C for 3 d and then slowly cooled to 25 °C at a rate of 5.8 °C h^{-1}. Colorless polyhedral crystals of **1** suitable for single-crystal X-ray structural determination were grown directly, separated manually, and dried in air (Yield: 50% based on the Dy^{III} salt). Anal. Calcd for $C_{16}H_{11}DyN_2O_5$: C, 40.56; H, 2.34; N, 5.91%. Found: C, 40.57; H, 2.32; N, 5.92%. IR (KBr, cm^{-1}): 3626 (w), 3047 (w), 1644 (s), 1619 (s), 1559 (s), 1467 (s), 1420 (s), 1382 (s), 1264 (w), 1160 (w), 1033 (m), 859 (m), 796 (m), 777 (m), 732 (w), 682 (m), 647 (m), 457 (w).

Synthesis of $[Yb(\mu_3\text{-OH})(na)(pyzc)]_n$ (2) and $[Gd(\mu_3\text{-OH})(na)(pyzc)]_n$ (3). Colorless block-shaped crystals of **2** and **3** were generated by adopting the procedures similar to those of **1** except that $Dy(NO_3)_3{\cdot}6H_2O$ was replaced, respectively, by $Yb(NO_3)_3{\cdot}6H_2O$ (for **2**) and $Gd(NO_3)_3{\cdot}6H_2O$ (for **3**). (Yield: 51% and 53% based on Yb^{III} and Gd^{III} salt, respectively). Anal. Calcd for $C_{16}H_{11}N_2O_5Yb$ (**2**): C, 39.68; H, 2.28; N, 5.78%. Found: C, 39.66; H, 2.32; N, 5.79%. IR

dx.doi.org/10.1021/ic501952b | Inorg. Chem. 2015, 54, 153−160

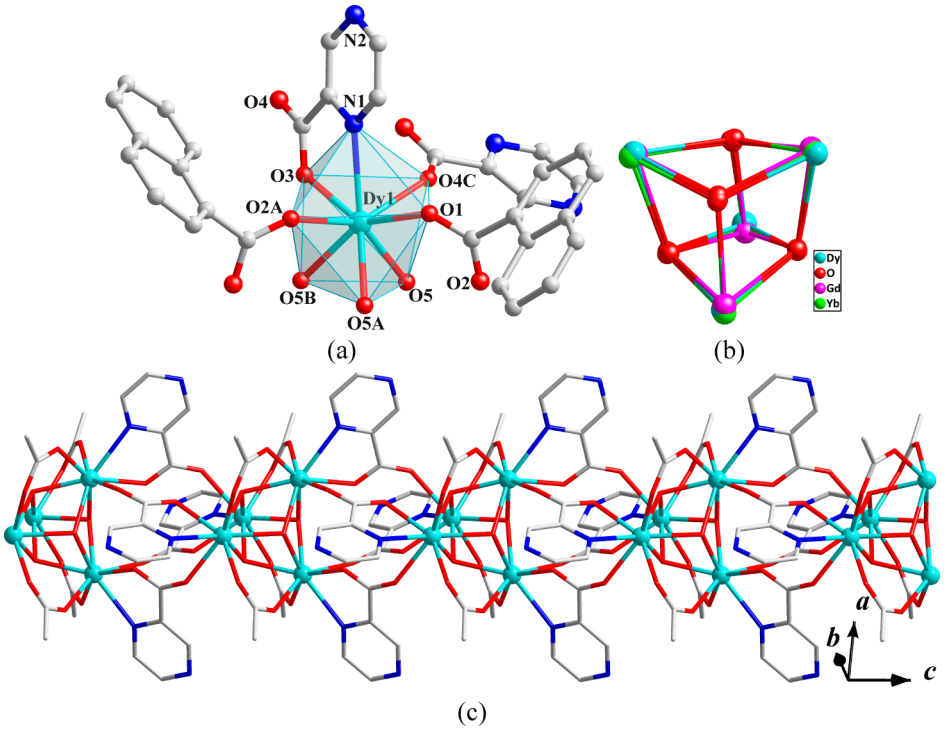

Figure 1. (a) Local coordination environment of Dy^{III} ions in **1** (hydrogen atoms were omitted for clarity, symmetry codes: A = $-x, y, -z$; B = $-x, -y, z$; C = $x, -y, 1-z$). (b) Superposition diagram of the three cubic $\{Ln_4O_4\}$ cores. (c) 1D chain of **1** constructed from the $\{Dy_4(\mu_3\text{-}OH)_4(\mu\text{-}COO)_4\}^{4+}$ clusters and $pyzc^-$ connectors.

(KBr, cm^{-1}): 3636 (w), 3050 (w), 1654 (s), 1625 (s), 1565 (s), 1464 (s), 1426 (s), 1381 (s), 1264 (m), 1160 (m), 1033 (m), 862 (m), 796 (m), 780 (m), 701 (m), 650 (m), 590 (w), 533 (w), 460 (w). Anal. Calcd for $C_{16}H_{11}GdN_2O_5$ (**3**): C, 41.02; H, 2.37; N, 5.98%. Found: C, 41.01; H, 2.36; N, 5.99%. IR (KBr, cm^{-1}) 3623 (w), 3044 (w), 1641 (s), 1619 (s), 1556 (s), 1467 (s), 1420 (s), 1381 (s), 1264 (m), 1160 (m), 1030 (m), 856 (m), 796 (m), 777 (m), 729 (m), 675 (w), 647 (w), 457 (w).

RESULTS AND DISCUSSION

Syntheses and IR Spectra. Complexes **1**−**3** with different rare earth ions were solvothermally synthesized with a molar ratio of 2:2:1 (Hna/Hpyzc/Ln^{III}) by tuning the pH value of the reaction medium and reaction temperature. Acting as a typically organic base, triethylamine was found to be more effective for both the pH control and crystal growth than inorganic NaOH. Additionally, the self-assembly processes carried out at the temperature lower than 170 °C only resulted in the tiny targeted microcrystals in a much lower yield, which were separated manually with much difficulty.

Weak and sharp absorptions at 3629 ± 9 cm^{-1} are resulting from the characteristic O−H stretching vibrations, suggesting the presence of hydroxyl group in **1**−**3** (Supporting Information, Figure S1). Weak absorptions at 3047 ± 3 cm^{-1} for **1**−**3** are associated with C−H stretch of the aromatic ring. As compared with the isolate carboxylate-containing ligand, a lack of characteristic band at 1675 or 1720 cm^{-1} indicates the deprotonation of the carboxylic acid.[25] Additionally, strong multiple bands for asymmetric and symmetric stretching vibrations of the $-COO^-$ moiety are clearly found at 1648 ± 6, 1622 ± 3, 1560 ± 5, 1465 ± 2, 1423 ± 3, as well as 1382 cm^{-1}, and their well overlaps may suggest the analogous binding manners of the carboxylate group in **1**−**3**. Apparently, the IR data well-sustain the structural determination results.

Crystal Structures of $[Ln(\mu_3\text{-}OH)(na)(pyzc)]_n$ (Ln = Dy (1), Yb (2), and Gd (3)). Complexes **1**−**3** are structurally identical, and they all crystallize from the tetragonal $I\bar{4}$ space group (Table 1), exhibiting linear one-dimensional (1D) chains with cubic $\{Dy_4(\mu_3\text{-}OH)_4(\mu\text{-}COO)_4\}^{4+}$ clusters extended by rigid $pyzc^-$ connectors. Because of their isostructural nature (Supporting Information, Figures S2−S4 and Tables S1−S3), only the representative structure of **1** is given herein with suitable comparisons with each other. The asymmetric unit of **1** includes a Dy^{III} cation, a $\mu_3\text{-}OH^-$ group, a monodeprotonated na^- ligand, as well as a deprotonated $pyzc^-$ anion. The sole Dy^{III} cation adopts a NO_7 donor set completed by one pyrazinyl N donor coming from the $pyzc^-$ ligand and seven oxygen atoms belonging to three $\mu_3\text{-}OH^-$ groups, four carboxylate groups from two pairs of symmetry-related na^- and $pyzc^-$ ligands (Figure 1a), exhibiting slightly distorted triangular dodecahedron coordination geometry. The Dy−O and Dy−N lengths are in the range of 2.320(4)−2.588(5) Å (Supporting Information, Table S1), which are normal to reported dysprosium analogues with 2,5-pyridine dicarboxylate ligand.[26]

Four symmetry-related $\mu_3\text{-}OH^-$ groups aggregate four separate Dy^{III} ions into a distorted cubic tetranuclear cluster with the intracluster metal−metal separations of 3.7561(2) to 3.7873(3) Å. The ∠DyODy of the cubic cluster varies from 106.150(2)° to 107.234(3)°, which are comparable to those dysprosium complexes showing SMM behaviors.[27] Additionally, the local $\{Dy_4(\mu_3\text{-}OH)_4\}^{8+}$ core is further encapsulated by four symmetry-related na^- anions through four bidentate bridging μ-*syn*, *syn*-COO^- groups (Figure 1b and Supporting Information, Scheme S1). Because of the different cation radius, the cubic clusters of **1**−**3** are slightly different each other (Supporting Information, Table S4), as shown in the superposition diagram of Figure 1b. Adjacent $\{Dy_4(\mu_3\text{-}$

dx.doi.org/10.1021/ic501952b | Inorg. Chem. 2015, 54, 153−160

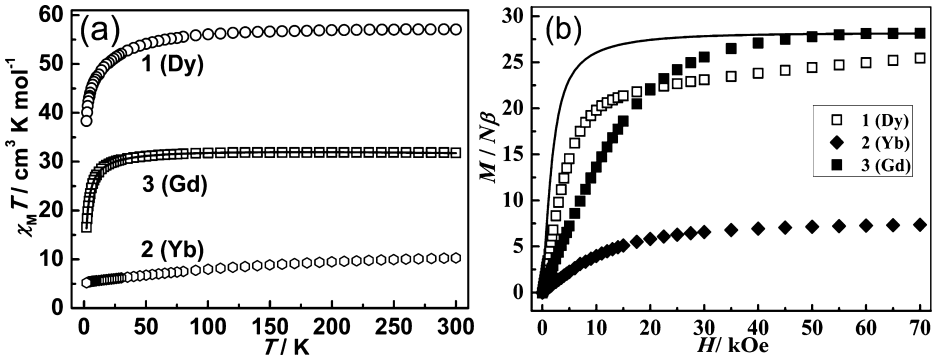

Figure 2. (a) Temperature dependence of the $\chi_M T$ for **1**−**3**. Solid line represents the best fit of the experimental data. (b) Field-dependent magnetizations for **1**−**3** at 2.0 K. The solid line represents the Brillouin function for four noninteracting Gd^{III} ions.

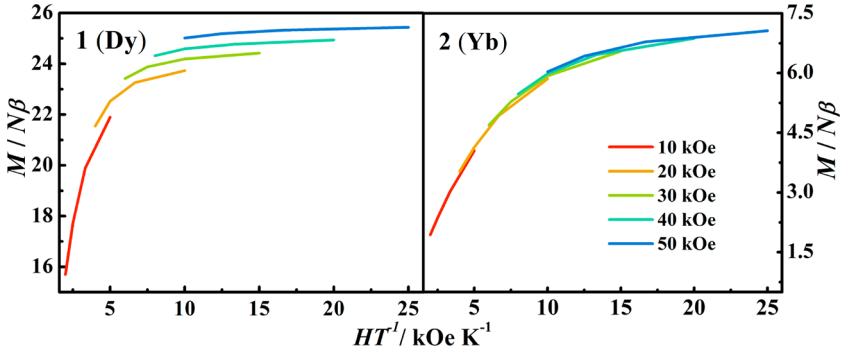

Figure 3. M vs H/T plots at different temperatures for **1** and **2**.

$OH)_4(\mu\text{-}COO)_4\}^{4+}$ cubanes in **1** are periodically extended by monodeprotonated chelating-bridging pyzc$^-$ connectors through the pyrizinyl N and two carboxylate O donors (μ-κ^3 N, O: O, Scheme S1), leading to a cubic cluster-based 1D array extending along the crystallographic c direction (Figure 1c) with the closest intercubic $Dy^{III}\cdots Dy^{III}$ distance of 6.1977(6) Å. The intercore intermetaallic separation is almost beyond the effective magnetic interacting distance. The infinite chains of **1** are further interacting with each other to a three-dimensional (3D) network by nonvalent C−H$\cdots\pi$ interactions from different aromatic rings (Figure S2).

PXRD Patterns and Thermogravimetric Analysis. Structural consistency and purity of the crystalline samples of **1**−**3** were examined by powder X-ray diffraction (PXRD) measurements (Supporting Information, Figure S5). The consistently experimental and computer-simulated patterns (Figure S5) evidenced that the bulk synthesized samples are homogeneous. In addition, the three samples can keep their compositional thermal stability before 350 °C and are accompanied by an obvious weight-loss process for the collapse of the polymeric frameworks (Supporting Information, Figure S6).

Magnetic Properties. Variable-temperature (300−2.0 K) magnetic susceptibilities were measured with an external field of 1 kOe for **1**−**3**. The observed $\chi_M T$ values for the Ln^{III}_4 cluster of **1** and **2** are 57.08 and 10.29 cm^3 K mol^{-1} at room temperature (Figure 2a), which are comparable to the expected values of 56.72 and 10.28 cm^3 K mol^{-1} for four magnetically noninteracting Dy^{III} and Yb^{III} ions. When the material is cooled, the $\chi_M T$ products of both entities decrease slowly to the lowest values of 38.2 (for **1**) and 5.31 (for **2**) cm^3 K mol^{-1} at 2.0 K. The decreasing $\chi_M T$ products are coming from the antiferromagnetic interactions of the rare earth ions within the tetranuclear unit, the progressively thermal depopulation of the ground-state Ln^{III} sublevels as well as the magnetic anisotropy,[28−30] which is hard to clearly distinguish each contribution.

The isothermal magnetizations of **1** and **2** recorded at 2.0 K (Figure 2b) display a rapid increase under low fields and then slowly approach the maxima of 25.44 and 7.35 Nβ at the highest field of 70 kOe. The maximum values are considerably smaller than the theoretical saturation values (40 and 16 Nβ) for four magnetically isolated Dy^{III} and Yb^{III} ions. The unsaturated magnetization together with the nonsuperimposed M versus H/T curves (Figure 3) suggest the existence of magnetic anisotropy and/or thermal population of the M_J sublevels in **1** and **2**.[31]

Magnetization dynamics of **1** and **2** were explored by alternating current (ac) susceptibility under a zero direct current (dc) field with an oscillation of 3.5 Oe. The frequency-dependent behavior to some different extent is observed for the imaginary ac signal (χ'') of **1** and **2** at the temperature lower than 10.0 K (Figure 4a), suggesting the appearance of slightly slow relaxation behavior of the magnetization.[32] Notably, the maximum value of the freqency-dependent χ'' signals of the two complexes can not be clearly detected probably due to the fast quantum tunnelling of magnetization (QTM), which can be essentially suppressed by supplying a dc magnetic field.[33] Therefore, dc field dependence of the χ'' singals for **1** and **2** were respectively scanned at 2.0 K and 1000 Hz to locate an optimized dc field (Supporting Information, Figures S7 and S8). The obtained results imply that a dc field of 3 kOe is enough for the effective suppression of the QTM process, which was thus applied to investigate the field-induced slow relaxation behavior of **1** and **2**. As shown in Figure 4b, a set of obvious frequency-dependent χ' and χ'' signals are clearly seen

dx.doi.org/10.1021/ic501952b | Inorg. Chem. 2015, 54, 153−160

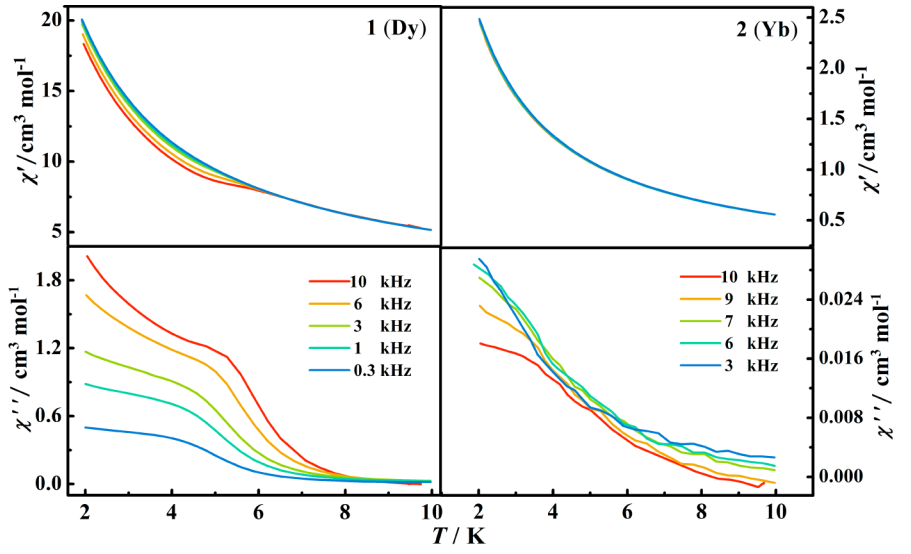

(a)

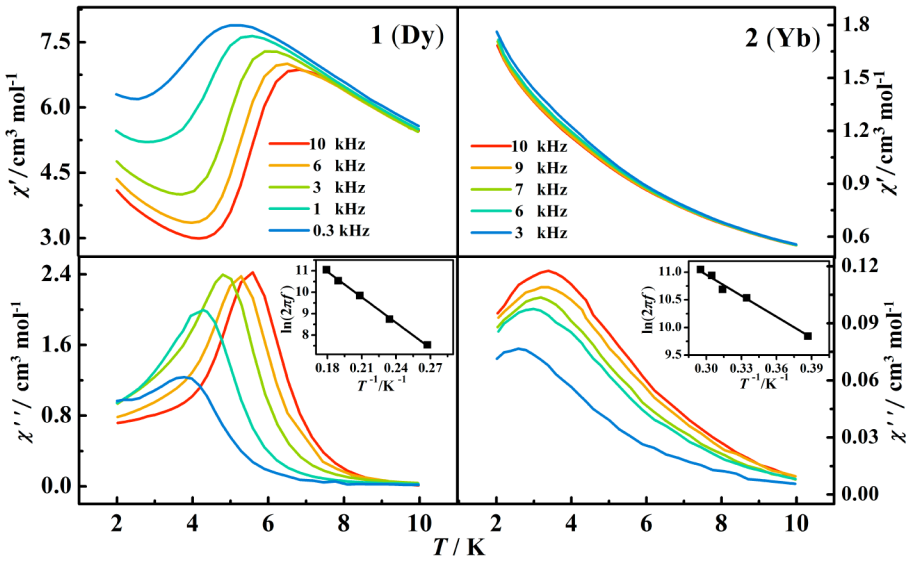

(b)

Figure 4. Temperature dependence of the in-phase (upper) and out-of-phase (lower) ac susceptibilities for **1** and **2** measured in a 3.5 *ac* field without (a) and with (b) a 3 kOe *dc* field. (inset) The solid lines represent the best fits to the Arrhenius law.

in the temperature ranges of 3.6 (0.3 kHz)−5.7 K (10 kHz) for **1** and 2.4 (3 kHz)−3.2 K(10 kHz) for **2**, indicating slow field-induced relaxation of magnetization. The Mydosh parameters estimated from this dependence, $\varphi = (\Delta T_p/T_p)/\Delta(\log f) = 0.38$ for **1** and 0.64 for **2** (T_p is defined as the maximum value of χ'' at different temperature),[9] is characteristic of normal superparamagnets, discarding spin-glass behavior.[34] Fitting the χ'' versus T data to Arrhenius law gives effective energy barrier $\Delta E/k_B = 39.6$ K and pre-exponential factor $\tau_o = 1.52 \times 10^{-8}$ s for **1** and $\Delta E/k_B = 14.1$ K, $\tau_o = 2.13 \times 10^{-7}$ s for **2**, which were shown in the inset of Figure 4b. Among diverse cubane-shaped {Dy_4} clusters, the energy barrier of **1** is lower than that of the reported values of $\Delta E/k_B = 73(2)$ K for $[Dy_4(L)_4(\mu_2\text{-}\eta^1\eta^1Piv)_4]\cdot 4H_2O\cdot 6CH_3OH$ (LH_2 = (*E*)-2-((6-(hydroxymethyl)pyridine-2-yl)methyleneamino)phenol and PivH = pivalic acid),[18] and higher than those of $[Dy_4(L)_4(\mu_4\text{-}OH)(\mu_3\text{-}OH)_2(NO_3)_4]\cdot(NO_3)\cdot 6CH_3CN\cdot H_2O$ (LH = 2-methoxy-6-(pyridin-2-ylhydrazonomethyl)phenol)[19] and $[Dy_4(\mu_3\text{-}OH)_2(\mu_3\text{-}O)_2(cpt)_6(MeOH)_6(H_2O)]_2\cdot 15MeOH$ (Hcpt =4-(4-carboxyphenyl)-1,2,4-triazole).[17] The τ_o values of **1** and **2** are consistent with the expected characteristic pre-exponential factor 10^{-6}−10^{-11} s for typical SMMs.[35−37] To the best of our knowledge, complex **2** is the first example showing slow magnetic relaxation among all the Yb^{III}-based complexes with cubane-shaped clusters.[28] The Cole−Cole plots (Supporting Information, Figure S9) show, in the temperature regions (3.6−4.8 K for **1** and 2.4−3.2 K for **2**), semicircular shapes with $0.18 > \alpha > 0.17$ (for **1**) and $0.20 > \alpha > 0.17$ (for **2**), revealing a narrow distribution of the relaxation time and a single relaxation mechanism. In addition, no obvious hysteresis

dx.doi.org/10.1021/ic501952b | *Inorg. Chem.* 2015, 54, 153−160

loops can be observed at 2.0 K for **1**−**2** due to their low block temperatures (Supporting Information, Figure S10).

For the isotropic Gd_4^{III}-based complex **3**, the $\chi_M T$ product is 31.80 cm^3 mol^{-1} K at 300 K (Figure 2a), close to the theoretical value (31.52 cm^3 mol^{-1} K) for four magnetically isolated Gd^{III} ions (S = 7/2, L = 0, g = 2). On lowering the temperature, the observed $\chi_M T$ value is almost invariable until ∼25 K. Upon further cooling, a fast decrease was seen to reach a value of 16.79 cm^3 K mol^{-1} at 2.0 K, which is most likely resulting from the intracluster antiferromagnetic exchange couplings between the spin carriers and/or zero-field splitting.[38,39] The local $\{Gd_4O_4\}$ core in **3** only slightly deviates from the perfect cubic with two pairs of comparable Gd^{III}···Gd^{III} distances (3.8078(2) and 3.8263(3) Å), the magnetic susceptibility of **3** thus can be approximately evaluated by the simplest one-J isotropic Hamiltonian $\boldsymbol{H} = -2J\ (\boldsymbol{S}_1\boldsymbol{S}_2 + \boldsymbol{S}_2\boldsymbol{S}_3 + \boldsymbol{S}_3\boldsymbol{S}_4 + \boldsymbol{S}_1\boldsymbol{S}_4)$. The fit of the experimental susceptibility data with the above equation, using the MAGPACK program,[40] affords the following parameters: J = −0.09 cm^{-1}, g = 2.01, and R = 3.2 × 10^{-2} (R is the agreement factor defined as $R = \Sigma[(\chi_M T)_{obsd} - (\chi_M T)_{calcd}]^2/\Sigma[(\chi_M T)_{obsd}]^2$). The obtained coupling constant is in good agreement with the reported values for other dihydroxy (J = −0.08 cm^{-1}), quinolinolate (J = −0.13 cm^{-1}), and diphenoxo (J = −0.09 cm^{-1})-bridged Gd^{III}-containing complexes.[18,29,41]

The isothermal M−H curve for each $\{Gd_4\}$ unit of **3** is well below the Brillouin function (Figure 2b), confirming weak antiferromagnetic interactions between the spin carriers. The magnetization of **3** is saturated at 70 kOe (28.14 $N\beta$), which is almost identical to the theoretical value (28.12 $N\beta$) for four individual Gd^{III} ions with g = 2.01.[42,43] No obvious hysteresis loop can be observed at 2.0 K for **3** (Figure S10).

Interestingly, the much weaker antiferromagnetic interaction, large spin ground state, as well as the relatively low molecular mass of **3** allow us to evaluate the MCE by applying the Maxwell equation $(\Delta S_m(T)_{\Delta H} = \int[\partial M(T,H)/\partial T]_H dH)$ to obtain the isothermal magnetic entropy changes $-\Delta S_m$ from the experimental magnetization data.[44] As shown in Figure 5, the observed $-\Delta S_m$ values increase with an increasing magnetic field and a decreasing temperature, getting to a maximum value of 30.0 J kg^{-1} K^{-1} at 2.5 K with an applied field change of 70 kOe. The expected maximum $-\Delta S_m$ value can be calculated from the equation $-\Delta S_m = N_{Gd} R \ln(2S_{Gd} + 1)$, where N_{Gd} is the number of Gd^{III} present per mole of **3**, giving the upper limit of 36.9 J kg^{-1} K^{-1}. Obviously, the experimental maximum of $-\Delta S_m$ is smaller than the theoretical one, which can be ascribed to the presence of an antiferromagnetic exchange among the Gd^{III} ions.[45]

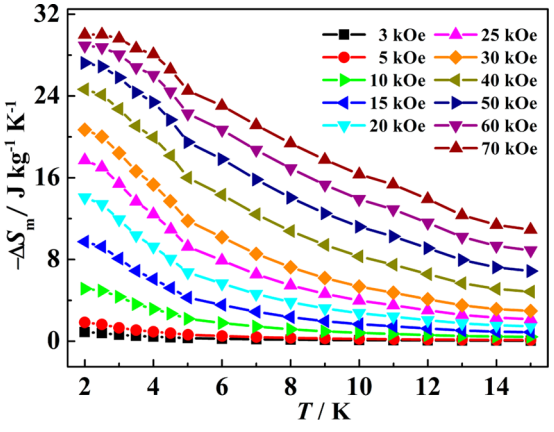

Figure 5. ΔS_m calculated by using the magnetization data of **3** at different fields and temperatures.

Photoluminescence. Functional ligand in the lanthanide complex can serve as excellent sensitizer to enhance the Ln^{III}-based luminescence via "antenna effect". Thus, solid-state photoluminescence spectra of **1**−**3**, together with free Hna and Hpyzc ligands, were investigated at ambient temperature to explore the photophysical behavior in the UV−visible region. As depicted in Figure 6, free Hna and Hpyzc species show

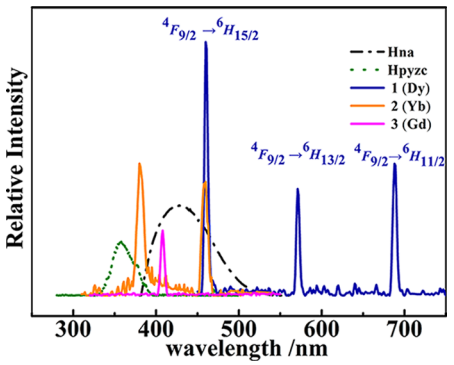

Figure 6. Solid-state fluorescence emissions of **1**−**3**, free Hna, and Hpyzc ligands at room temperature.

broad emissions, respectively, at 425 and 358 nm upon photoexcitation at 345 and 326 nm, which can be ascribed to the intraligand $\pi^* \rightarrow \pi$ or $\pi^* \rightarrow n$ transitions. Photoexcitation of **1** at 350 nm results in the observation of three characteristic bands at 460, 571, and 688 nm arising from $^4F_{9/2} \rightarrow {}^6H_{15/2}$, $^4F_{9/2} \rightarrow {}^6H_{13/2}$, and $^4F_{9/2} \rightarrow {}^6H_{11/2}$ transitions of the Dy^{III} center, respectively.[46] Upon excitation at 280 nm, complex **2** displays two relatively weak emissions at 380 and 458 nm, which may come from the charge transfer state to the $^2F_{7/2}$ and $^2F_{5/2}$, respectively. Obviously, the characteristic emissions for the mixed ligands were not observed in the two complexes, indicating that mixed Hna and Hpyzc can effectively transfer the energy to Dy^{III} and Yb^{III} centers during photoluminescence.

By contrast, upon excitation at 300 nm, compound **3** displays one emission at 407 nm, which is corresponding to ligand-to-ligand charge transfer. As compared with those of free Hna and Hpyzc organics, the apparent shift of the emission spectra of **3** is due to the nephelauxetic effect. The absence of the typical 4f → 4f emission of **3** suggests that the energy level from the intraligand electron transfer is too low to meet the requirement the lowest resonant energy level of Gd^{III} ion. The photoluminescence investigations of the three complexes mentioned above suggest that the mixed Hna and Hpyzc Hpyzc can act as an excellent antenna for effectively sensitizing the luminescence of Dy^{III} and Yb^{III} ions, which could be anticipated as potential fluorescent materials.

CONCLUSIONS

Facile self-assembly reactions of Ln^{III} ions with a combination of rigid 1-naphthoic acid and 2-pyrazinecarboxylic acid under solvothermally conditions generated three isostructural one-dimensional chains with slightly distorted cubane-like $\{Ln_4(\mu\text{-}OH)_4\}^{8+}$ cores (Ln = Dy (**1**), Yb (**2**), and Gd (**3**)). Significantly relying on the different single-ion anisotropies of the spin carriers, the former two complexes exhibit field-induced slow

dx.doi.org/10.1021/ic501952b | Inorg. Chem. 2015, 54, 153−160

relaxation of magnetization, with the anisotropy barriers of 39.6 and 14.1 K. Complex **3** with the isotropic Gd^{III} ion and weak antiferromagnetic coupling shows a significant cryogenic MCE, with a maximum entropy change of $-\Delta S_m = 30.0$ J kg^{-1} K^{-1} at 2.5 K and 70 kOe. Additionally, the luminescence behavior of **1**−**3** in the UV−visible region shows that the mixed carboxylate-functionalized aromatic ligands can efficiently divert the absorbed light energy to the Dy^{III} and Yb^{III} ions, thus strengthening the overall emission properties.

■ ASSOCIATED CONTENT

Supporting Information

Selected structural parameters and figures, conventional physical measurement results consisting of TG curves, IR spectra, PXRD patterns, hysteresis loops, dc/ac susceptibility for **1**−**3**, Cole−Cole plots for **1** and **2**, and X-ray crystallographic files in CIF format for **1**−**3**. This material is available free of charge via the Internet at http://pubs.acs.org. Crystallographic data for **1**−**3** have been assigned the CCDC numbers 1016277−1016279 by the Cambridge Crystallographic Data Centre.

■ AUTHOR INFORMATION

Corresponding Authors

*E-mail: encui_yang@163.com. (E.-C. Y.)

*E-mail: xiaojun_zhao15@163.com. (X.-J. Z.)

Notes

The authors declare no competing financial interest.

■ ACKNOWLEDGMENTS

We really appreciate the financial funds from the NSFC (Grant Nos. 21171129, 21173157, and 21371134), the 973 Program (2014CB845601), the Program for Innovative Research Team in University of Tianjin (TD12−5038), and Tianjin Municipal Education Commission (2012ZD02).

■ REFERENCES

(1) (a) Ardavan, A.; Rival, O.; Morton, J. J. L.; Blundell, S. J.; Tyryshkin, A. M.; Timco, G. A.; Winpenny, R. E. P. *Phys. Rev. Lett.* **2007**, *98*, 057201−057204. (b) Bogani, L.; Wernsdorfer, W. *Nat. Mater.* **2008**, *7*, 179−186. (c) Affronte, M. *J. Mater. Chem.* **2009**, *19*, 1731−1737. (d) Stamp, P. C. E.; Gaita-Arino, A. *J. Mater. Chem.* **2009**, *19*, 1718−1730. (e) Aromı, G.; Aguila, D.; Gamez, P.; Luis, F.; Roubeau, O. *Chem. Soc. Rev.* **2012**, *41*, 537−546.

(2) (a) Tuna, F.; Smith, C. A.; Bodensteiner, M.; Ungur, L.; Chibotaru, L. F.; Mcinnes, E. J. L.; Winpenny, R. E. P.; Collison, D.; Layfield, R. A. *Angew. Chem., Int. Ed.* **2012**, *51*, 6976−6980. (b) Mereacre, V. *Angew. Chem., Int. Ed.* **2012**, *51*, 9922−9925. (c) Colacio, E.; Ruiz, J.; Mota, A. J.; Palacios, M. A.; Cremades, E.; Ruiz, E.; White, F. J.; Brechin, E. K. *Inorg. Chem.* **2012**, *51*, 5857−5868. (d) Cucinotta, G.; Perfetti, M.; Luzon, J.; Etienne, M.; Car, P.-E.; Caneschi, A.; Calvez, G.; Bernot, K.; Sessoli, R. *Angew. Chem., Int. Ed.* **2012**, *51*, 1606−1610. (e) Liu, J.-L.; Guo, F.-S.; Meng, Z.-S.; Zheng, Y.-Z.; Leng, J.-D.; Tong, M.-L.; Ungur, L.; Chibotaru, L. F.; Heroux, K. J.; Hendrickson, D. N. *Chem. Sci.* **2011**, *2*, 1268−1272. (f) Yamashita, A.; Watanabe, A.; Akine, S.; Nabeshima, T.; Nakano, M.; Yamamura, T.; Kajiwara, T. *Angew. Chem., Int. Ed.* **2011**, *50*, 4016−4019.

(3) Liu, J.-L.; Chen, Y.-C.; Guo, F.-S.; Tong, M.-L. *Coord. Chem. Rev.* **2014**, *281*, 26−49.

(4) Bottrill, M.; Kwok, L.; Long, N. J. *Chem. Soc. Rev.* **2006**, *35*, 557−571.

(5) Xu, W.-T.; Zhou, Y.-F.; Huang, D.-C.; Xiong, W.; Su, M.-Y.; Wang, K.; Han, S.; Hong, M.-C. *Cryst. Growth Des.* **2013**, *13*, 5420−5432.

(6) Pedersen, K. S.; Lorusso, G.; Morales, J. J.; Weyhermüller, T.; Piligkos, S.; Singh, S. K.; Larsen, D.; Schau-Magnussen, M.; Rajaraman, G.; Evangelisti, M.; Bendix, J. *Angew. Chem., Int. Ed.* **2014**, *53*, 2394−2397.

(7) (a) Morimoto, M.; Miyasaka, H.; Yamashita, M.; Irie, M. *J. Am. Chem. Soc.* **2009**, *131*, 9823−9835. (b) Clemente-León, M.; Coronado, E.; Martí-Gastaldoz, C.; Romero, F. M. *Chem. Soc. Rev.* **2011**, *40*, 473−497. (c) Nihei, M.; Okamoto, Y.; Sekine, Y.; Hoshino, N.; Shiga, T.; Liu, I. P.-C.; Oshio, H. *Angew. Chem., Int. Ed.* **2012**, *51*, 6361−6364. (d) Blagg, R. J.; Tuna, F.; McInnes, E. J. L.; Winpenny, R. E. P. *Chem. Commun.* **2011**, *47*, 10587−10589.

(8) (a) Liu, S.-J.; Zhao, J.-P.; Song, W.-C.; Han, S.-D.; Liu, Z.-Y.; Bu, X.-H. *Inorg. Chem.* **2013**, *52*, 2103−2109. (b) Wang, B.-Wu; Jiang, S.-D.; Wang, X.-T.; Gao, S. *Sci. China, Ser. B: Chem.* **2009**, *52*, 1739−1758.

(9) (a) Guo, F. S.; Leng, J. D.; Liu, J. L.; Meng, Z. S.; Tong, M. L. *Inorg. Chem.* **2012**, *51*, 405−413. (b) Sharples, J. W.; Zheng, Y.-Z.; Tuna, F.; McInnes, E. J. L.; Collison, D. *Chem. Commun.* **2011**, *47*, 7650−7652. (c) Guo, F. S.; Chen, Y. C.; Mao, L. L.; Lin, W. Q.; Leng, J. D.; Tarasenko, R.; Orendáč, M.; Prokleška, J.; Sechovský, V.; Tong, M. L. *Chem.−Eur. J.* **2013**, *19*, 14876−14885. (d) Chang, L. X.; Xiong, G.; Wang, L.; Cheng, P.; Zhao, B. *Chem. Commun.* **2013**, *49*, 1055−1057. (e) Wu, M.; F. Jiang, F.; Kong, X.; Yuan, D.; Long, L.; Al-Thabaiti, S. A.; Hong, M. *Chem. Sci.* **2013**, *4*, 3104−3109.

(10) Liu, S.-J.; Zhao, J.-P.; Tao, J.; Jia, J.-M.; Han, S.-D.; Li, Y.; Chen, Y.-C.; Bu, X.-H. *Inorg. Chem.* **2013**, *52*, 9163−9165.

(11) (a) Meng, Y.; Chen, Y.-C.; Zhang, Z.-M.; Lin, Z.-J.; Tong, M.-L. *Inorg. Chem.* **2014**, *53*, 9052−9057. (b) Guo, F.-S.; Chen, Y.-C.; Liu, J.-L.; Leng, J.-D.; Meng, Z.-S.; Vrábel, P.; Orendáč, M.; Tong, M.-L. *Chem. Commun.* **2012**, *48*, 12219−12221.

(12) Rinehart, J. D.; Long, J. R. *Chem. Sci.* **2011**, *2*, 2078−2085.

(13) Sabbatini, N.; Guardigli, M.; Lehn, J.-M. *Coord. Chem. Rev.* **1993**, *123*, 201−228.

(14) Zhang, P.; Zhang, L.; Wang, C.; Xue, S.-F.; Lin, S.-Y.; Tang, J.-K. *J. Am. Chem. Soc.* **2014**, *136*, 4484−4487.

(15) Biswas, S.; Jena, H. S.; Adhikary, A.; Konar, S. *Inorg. Chem.* **2014**, *53*, 3926−3928.

(16) Saber, M. R.; Dunbar, K. R. *Chem. Commun.* **2014**, *50*, 2177−2179.

(17) Savard, D.; Lin, P. H.; Burchell, T. J.; Korobkov, I.; Wolfgang, W.; Clerac, R.; Murugesu, M. *Inorg. Chem.* **2009**, *48*, 11748−11754.

(18) Das, S.; Dey, A.; Biswas, S.; Colacio, E.; Chandrasekhar, V. *Inorg. Chem.* **2014**, *53*, 3417−3426.

(19) Goura, J.; Walsh, J. P. S; Tuna, F.; Chandrasekhar, V. *Inorg. Chem.* **2014**, *53*, 3385−3391.

(20) (a) Long, J.; Vallat, R.; Ferreira, R. A. S.; Carlos, L. D.; Paz, F. A. A.; Guari, Y.; Larionova, J. *Chem. Commun.* **2012**, *48*, 9974−9976. (b) Ren, M.; Bao, S.-S.; Ferreira, R. A. S.; Zheng, L.-M.; Carlos, L. D. *Chem. Commun.* **2014**, *50*, 7621−7624. (c) Zeng, D.; Ren, M.; Bao, S.-S.; Li, L.; Zheng, L.−M. *Chem. Commun.* **2014**, *50*, 8356−8359.

(21) Palacios, M. A.; Titos-Padilla, S.; Ruiz, J.; Herrera, J. M.; Pope, S. J. A.; Brechin, E. K.; Colacio, E. *Inorg. Chem.* **2014**, *53*, 465−1474.

(22) Sheldrick, G. M. *SADABS;* University of Göttingen: Göttingen, Germany, 1996.

(23) Bruker AXS. *SAINT software Reference Manual;* Bruker AXS Inc: Madison, WI, 1998.

(24) (a) Sheldrick, G. M. *SHELXL-97, Program for X-ray Crystal Structure Refinement;* Göttingen University: Göttingen, Germany, 1997. (b) Sheldrick, G. M. *SHELXS-97, Program for X-ray Crystal Structure Solution;* Göttingen University: Göttingen, Germany, 1997.

(25) Bellamy, L. J. *The Infrared Spectra of Complex Molecules;* Wiley: New York, 1958.

(26) Wang, C.-G.; Xing, Y.-H.; Li, Z.-P.; Li, J.; Zheng, X.-Q.; Ge, M.-F.; Niu, S.-Y. *Cryst. Growth Des.* **2009**, *9*, 1525−1530.

(27) Ke, H.; Gamez, P.; Zhao, L.; Xu, G.-F.; Xue, S.; Tang, J. *Inorg. Chem.* **2010**, *49*, 7549−7557.

(28) (a) Lin, P. H.; Sun, W. B.; Tian, Y. M.; Yan, P. F.; Ungur, L.; Chibotaru, L. F.; Murugesu, M. *Dalton Trans.* **2012**, *41*, 12349−12352.

(b) Pointillart, F.; Guennic, B. L.; Golhen, S.; Cador, O.; Maury, O.; Ouahab, L. *Chem. Commun.* **2013**, *49*, 615−617.
(29) Long, J.; Habib, F.; Lin, P. H.; Korobkov, I.; Enright, G.; Ungur, L.; Wernsdorfer, W.; Chibotaru, L. F.; Murugesu, M. *J. Am. Chem. Soc.* **2011**, *133*, 5319−5328.
(30) Abragam, A.; Bleaney, B. *Electron Paramagnetic Resonance of Transition Ions;* Dover Publications: New York, 1986.
(31) Xiang, H.; Lan, Y.-H.; Li, H.-Y.; Jiang, L.; Lu, T.-B.; Ansona, C. E.; Powell, A. K. *Dalton Trans.* **2010**, *39*, 4737−4739.
(32) Langley, S. K.; Moubaraki, B.; Murray, K. S. *Inorg. Chem.* **2012**, *51*, 3947−3949.
(33) Anwar, M. U.; Thompson, L. K.; Dawe, L. N.; Habib, F.; Murugesu, M. *Chem. Commun.* **2012**, *48*, 4576−4578.
(34) (a) Dong, D.-P.; Zhang, Y.-J.; Zheng, H.; Zhuang, P.-F.; Zhao, L.; Xu, Y.; Hu, J. X.; Liu, T.; Duan, C.-Y. *Dalton Trans.* **2013**, *42*, 7693−7698. (b) Zhou, N.; Ma, Y.; Wang, C.; Xu, G.-F.; Tang, J.-K.; Xu, J.-X.; Yan, S.-P.; Cheng, P.; Li, L.-C.; Liao, D.-Z. *Dalton Trans.* **2009**, 8489−8492. (c) Shi, P.-F.; Zheng, Y.-Z.; Zhao, X.-Q.; Xiong, G.; Zhao, B.; Cheng, P. *Chem.−Eur. J.* **2012**, *18*, 15086−15091.
(35) Mishra, A.; Wernsdorfer, W.; Abboud, A. K.; Christou, G. *J. Am. Chem. Soc.* **2004**, *126*, 15648−15649.
(36) Gatteschi, D.; Sessoli, R. *Angew. Chem., Int. Ed.* **2003**, *42*, 268−297.
(37) Shi, P.-F.; Xiong, G.; Zhao, B.; Zhang, Z.-Y.; Cheng, P. *Chem. Commun.* **2013**, *49*, 2338−2340.
(38) Zou, L.-F.; Zhao, L.; Guo, Y.-N.; Yu, G.-M.; Guo, Y.; Tang, J.-K.; Li, Y.-H. *Chem. Commun.* **2011**, *47*, 8659−8661.
(39) Kong, X. J.; Ren, Y. P.; Chen, W. X.; Long, L. S.; Zheng, Z.; Huang, R. B.; Zheng, L. S. *Angew. Chem., Int. Ed.* **2008**, *47*, 2398−2401.
(40) (a) Borrás-Almenar, J. J.; Clemente-Juan, J. M.; Coronado, E.; Tsukerblat, B. S. *Inorg. Chem.* **1999**, *38*, 6081−6088. (b) Borrás-Almenar, J. J.; Clemente-Juan, J. M.; Coronado, E.; Tsukerblat, B. S. *J. Comput. Chem.* **2001**, *22*, 985−991.
(41) Chandrasekhar, V.; Bag, P.; Colacio, E. *Inorg. Chem.* **2013**, *52*, 4562−4570.
(42) Woodruff, D. N.; Winpenny, R. E. P.; Layfield, R. A. *Chem. Rev.* **2013**, *113*, 5110−5148.
(43) Rinehart, J. D.; Long, J. R. *Chem. Sci.* **2011**, *2*, 2078−2085.
(44) Lorusso, G.; Palacios, M. A.; Nichol, G. S.; Brechin, E. K.; Roubeau, O.; Evangelisti, M. *Chem. Commun.* **2012**, *48*, 7592−7594.
(45) Chen, Y.-C.; Guo, F.-S.; Zheng, Y.-Z.; Liu, J.-L.; Leng, J.-D.; Tarasenko, R.; Orendáč, M.; Prokleška, J.; Sechovskỳ, V.; Tong, M.-L. *Chem.−Eur. J.* **2013**, *19*, 13504−13510.
(46) Li, Q.-W.; Liu, J.-L.; Jia, J.-H.; Leng, J.-D.; Lin, W.-Q.; Chen, Y.-C.; Tong, M.-L. *Dalton Trans.* **2013**, *42*, 11262−11270.